JACS
JOURNAL OF THE AMERICAN CHEMICAL SOCIETY

Article

pubs.acs.org/JACS

Alkyne-Tag SERS Screening and Identification of Small-Molecule-Binding Sites in Protein

Jun Ando,[†,‡,§,∥] Miwako Asanuma,[†,‡,§] Kosuke Dodo,[†,‡,§] Hiroyuki Yamakoshi,[‡,§] Satoshi Kawata,[∥] Katsumasa Fujita,[*,†,‡,∥] and Mikiko Sodeoka[*,†,‡,§]

[†]AMED-CREST, Japan Agency for Medical Research and Development, Saitama 351-0198, Japan
[‡]Sodeoka Live Cell Chemistry Project, ERATO, Japan Science and Technology Agency, Saitama 351-0198, Japan
[§]Synthetic Organic Chemistry Laboratory, RIKEN, Saitama 351-0198, Japan
[∥]Department of Applied Physics, Osaka University, Osaka 565-0871, Japan

Supporting Information

ABSTRACT: Identification of small-molecule-binding sites in protein is important for drug discovery and analysis of protein function. Modified amino-acid residue(s) can be identified by proteolytic cleavage followed by liquid chromatography−mass spectrometry (LC−MS), but this is often hindered by the complexity of the peptide mixtures. We have developed alkyne-tag Raman screening (ATRaS) for identifying binding sites. In ATRaS, small molecules are tagged with alkyne and form covalent bond with proteins. After proteolysis and HPLC, fractions containing the labeled peptides with alkyne tags are detected by means of surface-enhanced Raman scattering (SERS) using silver nanoparticles and sent to MS/MS to identify the binding site. The use of SERS realizes high sensitivity (detection limit: ∼100 femtomole) and reproducibility in the peptide screening. By using an automated ATRaS system, we successfully identified the inhibitor-binding site in cysteine protease cathepsin B, a potential drug target and prognostic marker for tumor metastasis. We further showed that the ATRaS system works for complex mixtures of trypsin-digested cell lysate. The ATRaS technology, which provides high molecular selectivity to LC−MS analysis, has potential to contribute in various research fields, such as drug discovery, proteomics, metabolomics and chemical biology.

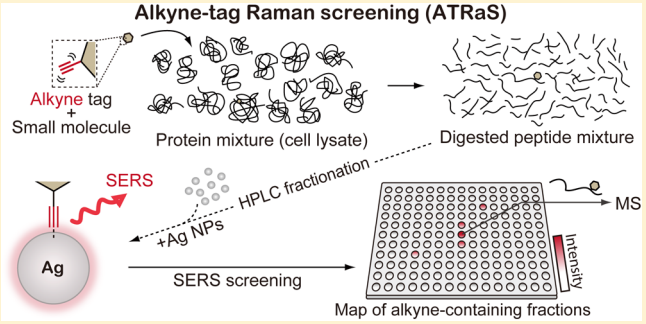

INTRODUCTION

The biological functions of proteins in cells can be modulated by chemical modification of the proteins with small molecules such as covalent drugs, as well as by physiological post-translational modifications. Thus, identification of sites in proteins that have been modified by small molecules is one of the key tasks in chemical biology research, since it provides insights into molecular mechanisms of action, specificity of protein binding, and biological functions.[1] Furthermore, activity-based probes, which are designed to covalently bond with the active sites of a group of enzymes, have been developed and used for the analysis of active enzymes in the proteome.[2] Mass spectrometry coupled with liquid chromatography (LC−MS) has been used to find small-molecule-binding peptides in proteolytic digests and to identify the modified residue(s) based on mass shift.[2] However, the complexity and dynamic range of HPLC-fractionated protein digests, which contain large amounts of unmodified peptides, often hinder the analysis.[3,4] A priori information, such as the mass shift induced by the modification, is required to analyze the vast amount of data automatically, but it is difficult to predict the mass shift precisely, if unexpected reaction and/or ionization occur. Moreover, small-molecule-modified peptides may require nonstandard ionization conditions in MS analysis. Therefore, an alternative approach that could identify specific LC fractions of a complex proteolytic mixture that contain peptides modified with small molecules, without relying on mass information, would be extremely useful. An efficient approach to specifically detect the small-molecule-labeled peptide in LC−MS analysis is to introduce a tag such as a radioisotope (RI) and fluorophore to the small molecule.[5] However, an RI tag requires special facilities and sample handling. A fluorophore enables specific detection of the target, but these tags are large in size and often reduce the binding affinity of the molecule. Thus, there is a need for a novel strategy to screen modified peptides without the use of RI or fluorescence.

Recently we demonstrated that alkyne-tagged small molecules in live cells could be directly visualized by using Raman microscope (alkyne-tag Raman imaging, ATRI).[6] Alkyne exhibits a Raman peak distinct from typical biological molecules and, therefore, can be specifically identified by Raman

Received: June 13, 2016
Published: October 10, 2016

DOI: 10.1021/jacs.6b06003
J. Am. Chem. Soc. 2016, 138, 13901−13910

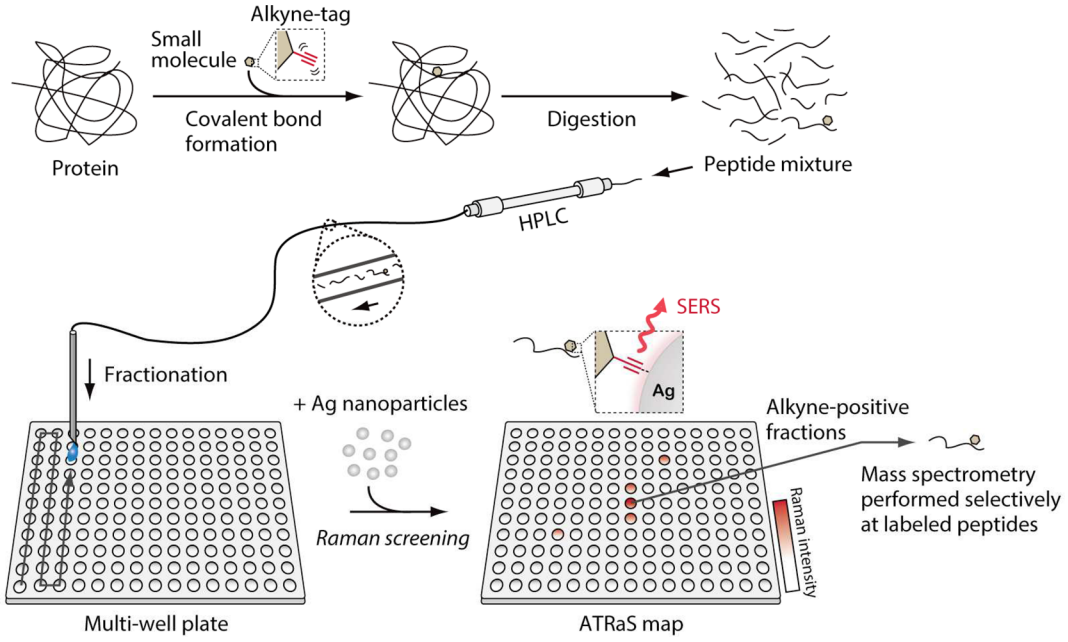

Figure 1. Schematic illustration of Alkyne-Tag Raman Screening (ATRaS) analysis to explore the HPLC fractions of a protein digest containing target peptides modified with alkyne-tagged small molecules. Positive fractions are analyzed by mass spectrometry to identify small-molecule-binding site(s) on the protein. Silver nanoparticles are added to the HPLC fractions to generate surface-enhanced Raman scattering (SERS) from the alkyne tag.

scattering. Alkyne is much smaller than typical fluorescence labels and has minimum effect on the binding capability of small molecules. Therefore, alkyne could be used as a tag for searching small-molecule-modified peptides in LC−MS analysis. But the very weak signal of Raman scattering prevented its use as a practical detection method for screening of a specific molecule in the diluted solution such as LC fraction.

We discovered that the combination of alkyne-tag and surface-enhanced Raman scattering (SERS)[7] detection realizes high sensitivity and reproducibility in peptide screening, which expedites the identification of small-molecule-binding sites in protein. Here, we report the details of the SERS-based alkyne-tag Raman screening (ATRaS).

RESULTS

The Scheme of ATRaS. Overview of ATRaS, utilized for the identification of amino acid residue(s) covalently modified by a small molecule in protein, is shown in Figure 1. The small molecule is tagged with alkyne and covalently bound to the target protein. The tagged protein is enzymatically digested to afford peptide fragments that are fractionated by HPLC. The fractions are collected on a multiwell plate by a fraction collector and analyzed by SERS. The extraordinarily strong enhancement of the terminal alkyne signal by silver nanoparticles enables the detection of alkyne-tagged molecules in the eluates with sufficiently high sensitivity. The SERS analysis enables mapping of alkyne-containing fractions on the plate, and MS analysis focused on these fractions containing alkyne-tagged peptides allows efficient determination of the modified amino acid residue(s).

SERS Detection of Alkyne Tags. To optimize the experimental conditions for ATRaS, we first investigated alkyne-modified peptides as models of proteolytic fragments bearing an alkyne-tagged small molecule. We prepared two synthetic peptides consisting of a 10-amino-acid sequence including propargyl glycine (alkyne-tagged peptide, alt-pept) or isoleucine (pept) (Figure 2a). Solution of each peptide (0.67 μM) was mixed with 40 nm silver nanoparticles, and their spectra were measured using a Raman microscope with a 532

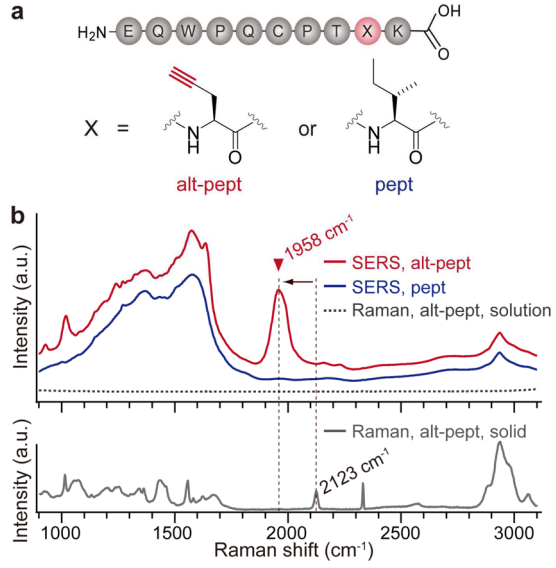

Figure 2. SERS detection of alkyne-tagged peptide. (a) Synthetic peptide EQWPQCPTXK (alt-pept: X = propargyl glycine, pept: X = isoleucine). Propargyl-glycine includes the alkyne moiety (red). (b) SERS spectra of 10 pmol alt-pept and pept, obtained with 40 nm silver nanoparticles, and Raman spectrum of 10 pmol alt-pept without silver nanoparticles (upper panel). In the SERS spectrum of alt-pept, the Raman peak of alkyne is observed at 1958 cm^{-1}, indicated by a red triangle. Raman spectrum of 1 nmol alt-pept in solid condition was also shown (lower panel), which was obtained from peptide aggregation of alt-pept, formed by solvent evaporation of peptide solution deposited on the substrate. Raman peak of alkyne is observed at 2123 cm^{-1}.

DOI: 10.1021/jacs.6b06003
J. Am. Chem. Soc. 2016, 138, 13901−13910

nm excitation laser. In the SERS spectrum of alt-pept, a strong Raman peak assigned to alkyne was found at 1958 cm^{-1}, while no such peak was detected from the solution of pept (Figure 2b). Since this peak appears in the Raman-silent window, selective detection of alkyne can be achieved irrespective of background Raman signals from other molecular vibrations. Although there are various types of molecular structures in alt-pept, such as the peptide backbone and functional groups in amino-acid residues, the SERS signal of alkyne was much stronger than the others, presumably due to high affinity of the alkyne group for the metal surface.[8] Adsorption of alkyne on the nanoparticles facilitates efficient amplification of the SERS signal, owing to charge-transfer-mediated chemical enhancement and localization of molecules within the enhanced optical field. The observed peak at 1958 cm^{-1} shows peak broadening and downshifting compared with the peak in a typical Raman spectrum (Figure 2b), indicating adsorption of alkyne on the silver surface.[9] It is noteworthy that no signal was detected for the diluted solution of alt-pept in the absence of silver nanoparticle (Figure 2b, dotted line). These results confirmed the strong SERS activity of alkyne and its detectability in peptide with high sensitivity and selectivity.

During the above study, we found that addition of trifluoroacetic acid (TFA) is critical to ensure high reproducibility and sensitivity of SERS detection. TFA induces stable aggregation of silver nanoparticles and peptides (Figure 3a), promoting uniform distribution on the glass substrate (Figure 3b; Figure S1 and S2, Supporting Information), and this enables quantitative SERS analysis of the aggregates.[10] In the absence of TFA, we observed large variations in SERS signal intensity among aggregates due to floating and inhomogeneous distribution of aggregates (Figure 3c and d). In contrast, TFA effectively suppressed the SERS intensity variation among measurement in different wells (Figure 3c and d; Figure S3 and S4, Supporting Information). We used line-shaped laser illumination for SERS excitation to measure Raman spectra from multiple aggregates simultaneously;[11] this improves the accuracy of measurement by averaging the SERS spectra from multiple aggregates with different sizes and shapes (Figure S5, Supporting Information). The TFA-promoted uniform aggregate formation on the surface of the glass substrate also enabled us to develop an automated ATRaS system.

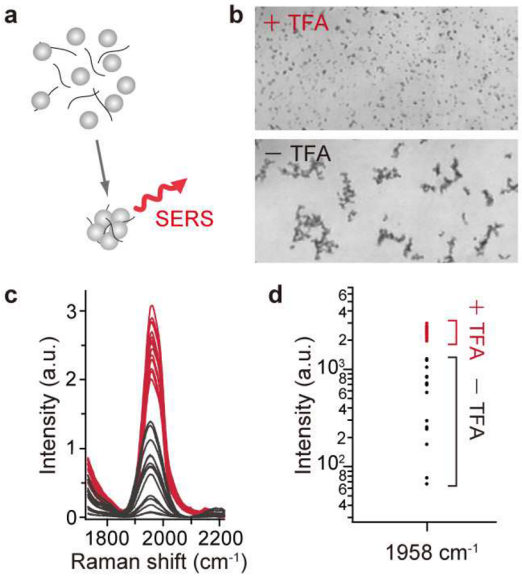

Figure 3. Effects of TFA on SERS detection of alkyne. (a) Illustration of silver nanoparticle aggregate formation together with peptides. The aggregates efficiently produce a SERS signal. (b) Bright-field images of aggregated silver nanoparticles with and without TFA, in the presence of alt-pept. With TFA, aggregates show a uniform distribution. (c) SERS spectra of 10 pmol alt-pept with TFA (red), and without TFA (black). Each spectrum was obtained from a different sample prepared in a separate well (n = 15). (d) Peak height of alt-pept at 1958 cm^{-1} with and without TFA, obtained from (c).

Sensitivity of ATRaS System. Typical sensitivity range of protein analysis with MS is femtomole level in terms of loading amount.[4] We therefore examined the detection limit of alt-pept with alkyne SERS, by measuring SERS signal intensity from samples containing different amounts of alt-pept (Figure 4; Figure S6 and S7, Supporting Information). The detection limit was 100 fmol, corresponding to 3.3 nM concentration (Figure 4; Figure S8, Supporting Information). Without silver nanoparticles, Raman peak of alt-pept in solution was not observed even at 10 mM concentration under the same measurement condition used for SERS detection (Figure S9, Supporting Information). Thus, SERS detection offers more than 6 orders of magnitude higher sensitivity than normal Raman spectroscopy. Quantitative alkyne detection is possible between 100 fmol and 100 pmol, where SERS intensity shows good proportionality to alt-pept loading (Figure 4; Figure S6 and S7, Supporting Information). When the loading amount was more than 100 pmol, the SERS intensity decreased and large intensity deviations appeared (Figure S6, Supporting Information), apparently because the nanoparticle aggregation was disturbed by excess peptide (Figure S10, Supporting Information). In the absence of TFA, SERS intensity was not proportional to alt-pept loading, and the detection sensitivity was more than 1 order of magnitude lower (Figure S11, Supporting Information). We also examined the dependence of the size, batch, and metal species of the nanoparticle on alkyne SERS measurement (Figure S12, Supporting Information). Comparable results were obtained when using 60 and 80 nm silver nanoparticles. In contrast, when nanoparticles smaller than 20 nm were used, apparent intensity decrease was observed. No significant variation of the peak intensity was observed among the different batches of 40 nm silver nanoparticles. When gold nanoparticles were used instead of silver, no signal was observed.

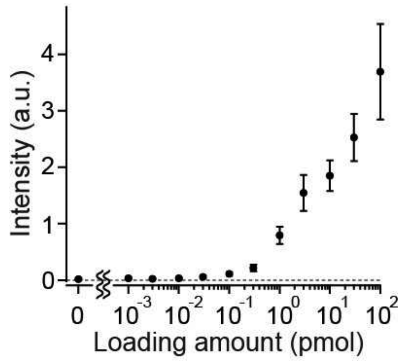

Figure 4. Relationship between the loading amount and the alkyne peak height of alt-pept with SERS. The detection limit is around 100 fmol.

DOI: 10.1021/jacs.6b06003
J. Am. Chem. Soc. 2016, 138, 13901−13910

HPLC-fractionated alt-pept was also analyzed by SERS. The SERS chromatogram, reconstructed from measurements of alkyne peak intensity, corresponded to the profile in the chromatogram obtained with UV detection (Figure S13, Supporting Information). When a mixture of alt-pept and pept was examined, the SERS chromatogram showed a single major peak corresponding to alt-pept, while the UV chromatogram showed two distinct major peaks (Figure 5; Figure S14, Supporting Information). It was confirmed that 300 fmol of alt-pept was within the detection range in the HPLC experiment (Figure S15, Supporting Information). We also checked the influence of acetonitrile on alkyne SERS measurement, since it can coordinate to transition metals and is commonly included in the HPLC solvent (Figure S16, Supporting Information). When the acetonitrile concentration was below 3% in solution, no significant intensity decrease was observed. In the ATRaS measurement, acetonitrile concentration in each fraction is less than 0.3%. Therefore, we confirmed that the presence of acetonitrile does not affect our measurement.

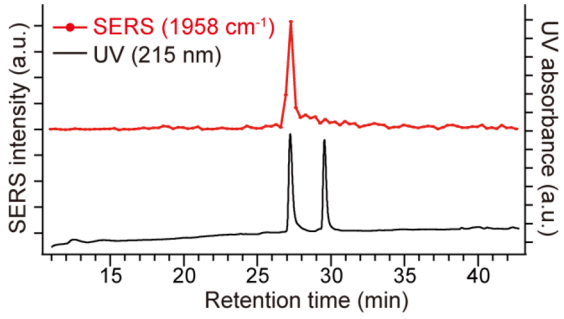

Figure 5. SERS and UV chromatograms of HPLC-fractionated alt-pept and pept mixture (10 pmol). The SERS chromatogram was reconstructed from the peak height of alkyne at 1958 cm^{-1}.

Identification of Inhibitor-Binding Site in Protein. We applied ATRaS to identify the inhibitor-binding site and specificity in the lysosomal cysteine protease cathepsin B (CatB). CatB has been widely investigated as a potential drug target and prognostic marker for tumor metastasis,[12] owing to its involvement in cancer progression.[13] An inhibitor peptide bearing an acyloxymethyl ketone (AOMK) group shows promise for clinical application due to its selective interaction with cysteine protease.[14] We focused on the CatB-selective inhibitor Z-FG-AOMK, developed by Bogyo and his colleagues (Figure 6a).[15a] Although numerous AOMK-type inhibitors have been developed and are believed to form a covalent bond selectively with the catalytic site cysteine residue (Figure 6b),[16] the modification site of Z-FG-AOMK in CatB has not been determined. Therefore, we selected Z-FG-AOMK for study with ATRaS, and synthesized alkyne-tagged Z-FG-AOMK, termed Alt-AOMK (Figure 6a; Scheme S1, Supporting Information). The inhibitory activity toward CatB was basically unchanged (Z-FG-AOMK: 1.0 μM, Alt-AOMK: 1.0 μM), indicating that the alkyne tag is small enough to have little effect on the binding affinity. In the presence of silver nanoparticles, Alt-AOMK showed a strong SERS peak at 1981 cm^{-1}, attributed to alkyne stretching vibrational mode (Figure 6c). We used this compound to label CatB (Figure 6d), and the labeled CatB was digested with trypsin. Cysteine residues were reduced and alkylated with iodoacetamide, and the peptide mixture was fractionated by HPLC. A fraction collector was used to fractionate the eluates into wells of a glass-bottomed 384-well plate at 20-s intervals.

Next, the 384-well plate array was examined by ATRaS and a SERS chromatogram was reconstructed based on the alkyne-peak intensity at 1981 cm^{-1} obtained from each fraction (Figure 6e). A UV chromatogram was also obtained during the HPLC fractionation (Figure 6e). Total screening time for ATRaS was 38 min for 192 fractions (exposure time for SERS detection was 3 s per sample). The SERS chromatogram showed a few major peaks at around the retention time of 52 min. The UV chromatogram, on the other hand, showed ubiquitous multiple peaks. It is especially noteworthy that the ATRaS system presented here is fully automated (Figure S17, Supporting Information).

An ATRaS map (Figure 6f) reconstructed from the alkyne Raman intensity measurements indicated that fractions #96 and 98 were appropriate target fractions for subsequent mass spectrometric analysis. We performed ESI-MS analysis of the same set of fractionated samples as used for SERS measurement that did not contain silver nanoparticles (Figures S18, Supporting Information). From the obtained mass spectra, we identified two peptides, which are labeled with Alt-AOMK, containing the same sequence ^{22}DQGSCGSCWAFG-AVEAISDR[41], with different cleavage positions (Figure 6g, Table 1 and Figure S19, Supporting Information). We also analyzed some SERS-negative fractions, shown in black in Figure 6f, and we did not find any other peptides, which were labeled with Alt-AOMK. These results indicate that the inhibitor selectively modified one of the amino acid residues of the peptide sequence. Further MS/MS analysis identified the residue, which was labeled with Alt-AOMK, as C^{29} (Figure S20, Table S1). These facts confirmed that Alt-AOMK binds catalytic site cysteine residue selectively.

We examined the detection limit of Alt-AOMK-modified CatB with ATRaS, by changing the loading amount of protein in HPLC (Figure S21, Supporting Information). Exposure time for SERS detection was 5 s per sample. SERS chromatogram was reconstructed using alkyne peak intensity at 1981 cm^{-1}. It was confirmed that 0.01 μg (~360 fmol) of Alt-AOMK-modified CatB was within the detection range.

Recently, detection of alkyne is widely performed by using ligation chemistry using cycloaddition of alkyne and azide, known as click chemistry.[17] Therefore, we compared ATRaS with click chemistry using a commercially available azide-modified fluorophore. Click reaction of CatB, which was labeled with Alt-AOMK, and subsequent purification were performed according to the standard protocol (Figure S22 and S23, Supporting Information), and the sample was digested and fractionated by HPLC in the same manner as above. Substantial sample loss of 59−76% occurred during click reaction and purification (Figure S24, Supporting Information). The fluorescence chromatogram also showed a broader intensity profile as compared with ATRaS (Figure 7; Figure S25, Supporting Information), probably due to the increased miscleavage or change of physical properties by the introduction of the large fluorophore. We could not detect the peptides, which was labeled with Alt-AOMK, by MS analysis with searching algorithm (MASCOT search) using expected mass shift (Figure S22, Supporting Information). Possible reasons for this failure include sample loss, decreased ionization efficiency and mass shift due to unexpected reaction. By virtue of direct alkyne detection, ATRaS avoids such problems, which might otherwise require extensive exper-

DOI: 10.1021/jacs.6b06003
J. Am. Chem. Soc. 2016, 138, 13901−13910

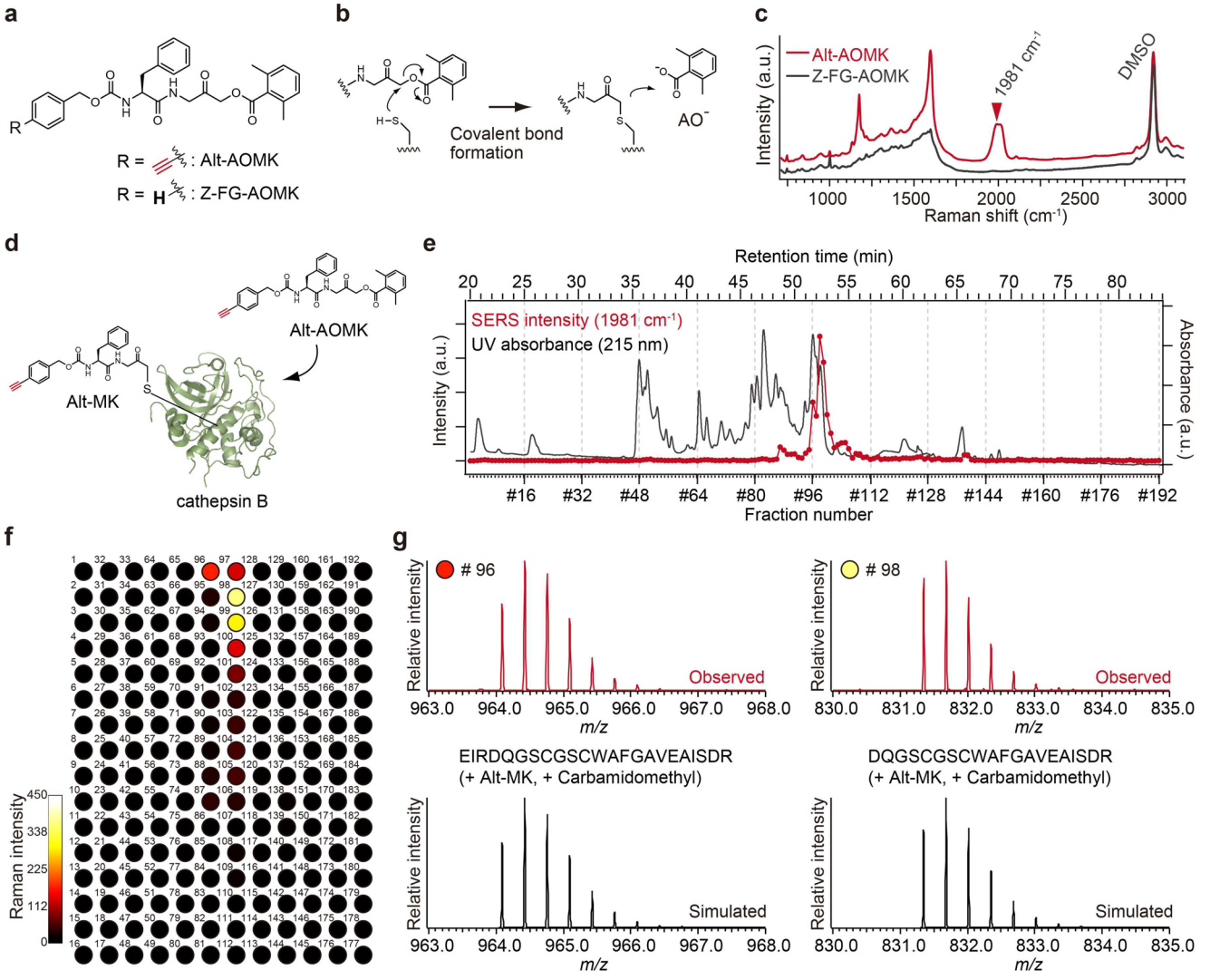

Figure 6. ATRaS for identification of inhibitor-binding site in cathepsin B (CatB). (a) Molecular structure of Z-FG-AOMK, a selective inhibitor of CatB,[15a] and its alkyne-modified derivative, Alt-AOMK. (b) Proposed covalent bond-forming reaction of AOMK-type inhibitor with cysteine protease. (c) SERS spectra of Alt-AOMK and Z-FG-AOMK with 40 nm silver nanoparticles. The peak at 1981 cm^{-1} of Alt-AOMK is a characteristic vibrational mode of alkyne. (d) Schematic illustration of CatB treatment with Alt-AOMK. (e) UV and SERS chromatograms of trypsin-digested CatB treated with Alt-AOMK. UV absorbance was monitored after HPLC-fractionation. The eluates were collected as an array in a glass-bottomed 384-well plate with fraction intervals of 20 s. The SERS chromatogram was reconstructed from the intensity profile of the alkyne peak at 1981 cm^{-1}. (f) SERS intensity map of alkyne overlaid on the multiwell plate, termed ATRaS map. (g) Major peaks of the electrospray ionization (ESI)-MS spectra obtained from fraction number 96 and 98 selected based on the ATRaS map (Figure 6f). Simulated MS spectra of $[M+3H]^{3+}$ of ^{19}EIRDQGSCGSCWAFGAVEAISDR[41] and ^{22}DQGSCGSCWAFGAVEAISDR[41], which are labeled with Alt-AOMK, are also displayed in the figure and Table 1.

Table 1. List of Peptides Detected by MS in Target Fractions Selected from the ATRaS Map[a]

fraction #	sequence position	sequence	theoretical mass (Da)	modification on Cys	theoretical $[M+3H]^{3+}(m/z)$	observed $[M+3H]^{3+}(m/z)$	m/z error (ppm)
96	22−41	DQGSCGSCWAFGAVEAISDR	2491.0209	CAM, Alt-MK	831.3476	831.3485	1.083
	19−41	EIRDQGSCGSCWAFGAVEAISDR	2889.2487	CAM, Alt-MK	964.0902	964.0911	0.934
98	22−41	DQGSCGSCWAFGAVEAISDR	2491.0209	CAM, Alt-MK	831.3476	831.3482	0.722
	19−41	EIRDQGSCGSCWAFGAVEAISDR	2889.2487	CAM, Alt-MK	964.0902	964.0922	2.074

[a]Underbars in the sequence indicate the positions of modified residues. CAM is the abbreviation for carbamidomethylation.

imental optimization to overcome, and has advantages in screening of peptides modified with small molecules.

ATRaS was then performed with cell lysate containing cathepsin B, to examine its applicability in complex proteolytic mixtures. We prepared cell lysate by solubilizing HL-60 cells in a buffer solution and adding a small amount (1/10 of total proteins) of cathepsin B. The sample solution was treated with Alt-AOMK, and the whole proteins were digested with trypsin. The resultant peptide mixture was fractionated by HPLC for subsequent ATRaS measurement. The SERS chromatogram showed a few major peaks; on the other hand, the UV chromatogram showed huge numbers of peaks (Figure 8a). An

DOI: 10.1021/jacs.6b06003
J. Am. Chem. Soc. 2016, 138, 13901−13910

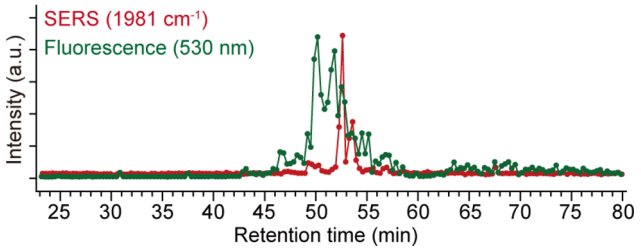

Figure 7. Comparison of SERS and fluorescence chromatograms of the mixture of peptide fragments from Alt-AOMK-treated CatB without or with click reaction using Alexa Fluor 488 Azide.

ATRaS map reconstructed from the alkyne Raman intensity measurements indicated that fraction #205 is an appropriate target fraction for subsequent mass spectrometry analysis (Figure 8b). We analyzed the target fraction with MALDI mass spectrometry, by collecting precipitated sample on the glass substrate (Figure S26, Supporting Information). From the obtained mass spectra, we identified the peptide modified with Alt-AOMK, which has same sequence discussed above (Figure 8c). This result confirms that ATRaS is effective in analysis of complex peptide mixtures.

Furthermore, to examine the limit of detectable peptide concentration, we performed ATRaS-MALDI-MS experiments of the cell lysate with decreased amounts of CatB (1/50−1/100 of the cell proteins). It was confirmed that the Raman signal and the MS signal of the modified peptide were detected even in the experiment using the protein mixture containing 1/100 CatB (Figure S27, Supporting Information). It is noteworthy that direct analysis of the original sample solution by MALDI-MS or LC−MS failed to detect the modified peptide using the protein mixture containing 1/100 CatB, which might be due to the limitation of dynamic range of the mass spectrometer (Figure S28 and S29, Supporting Information).

We also applied ATRaS to investigate the chemical reactivity of Alt-AOMK toward other cathepsin family enzymes: cathepsin L (CatL) and cathepsin S (CatS). Since their catalytic site structures are similar to CatB, Alt-AOMK is expected to bind to these enzymes and to react with the catalytic site cysteine residue. Indeed, Alt-AOMK inhibited CatL and CatS with the IC_{50} of 0.95 μM and 2.9 μM, respectively. Since the IC_{50} value for CatL is similar to that for CatB, we assumed that Alt-AOMK reacts with the catalytic site cysteine residue of CatL similarly. Thus, we performed ATRaS for both CatB and CatL treated with Alt-AOMK under the same conditions and compared the results. Unexpectedly, however, alkyne-SERS intensity of the Alt-AOMK-modified peptide derived from CatL was very weak (more than 46 times lower than that of the sample derived from CatB) (Figure S30, Supporting Information), indicating that efficiency of the covalent bond-formation with CatL is more than 1 order of magnitude lower than that with CatB, despite the fact that their IC_{50} values are similar. We also analyzed CatS-Alt-AOMK

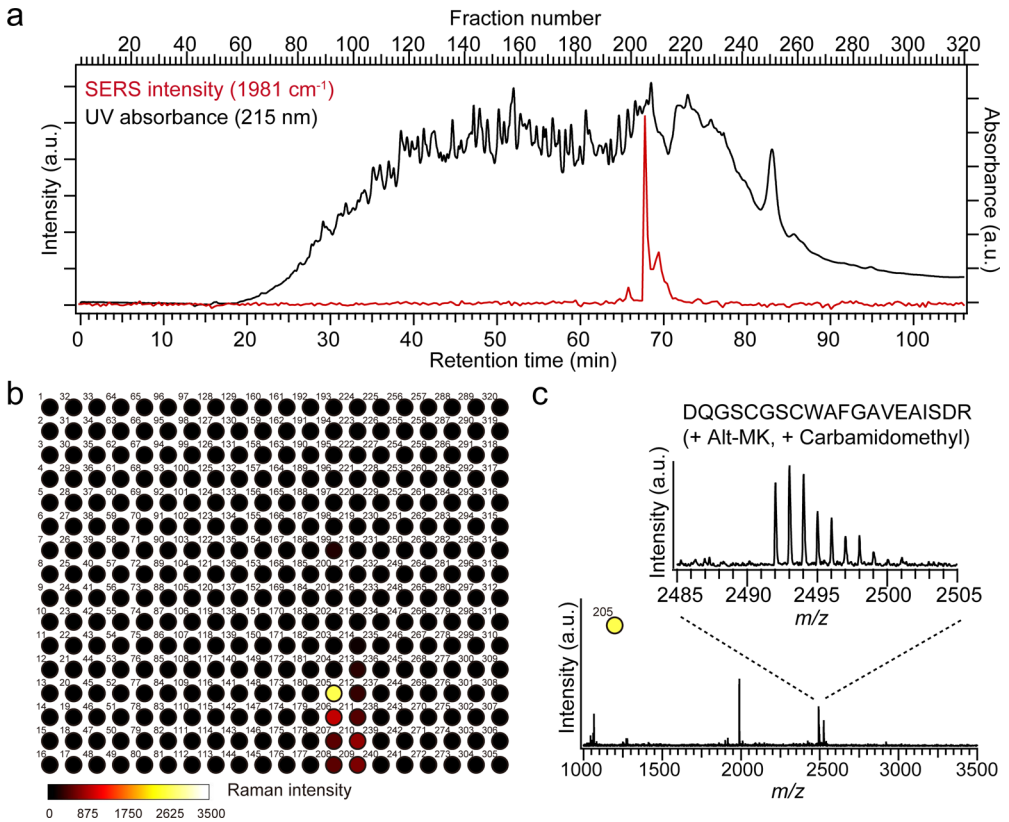

Figure 8. ATRaS for the analysis of CatB in cell lysate. (a) UV and SERS chromatograms of tryptic digest of the Alt-AOMK-treated cell lysate containing CatB (a tenth part of the total proteins). The protein mixture was treated with Alt-AOMK, and digested by trypsin. UV absorbance was monitored after HPLC-fractionation. The eluates were collected as an array in a glass-bottomed 384-well plate with fraction intervals of 20 s. The SERS chromatogram was reconstructed from the intensity profile of the alkyne peak at 1981 cm^{-1}. (b) ATRaS map reconstructed from the SERS intensity in (a). (c) MALDI-TOF MS spectrum of fraction number 205 selected based on the ATRaS map (b). Ions corresponding to the $[M + H]^+$ of the Alt-AOMK-labeled ^{22}DQGSCGSCWAFGAVEAISDR^{41} are observed.

DOI: 10.1021/jacs.6b06003
J. Am. Chem. Soc. 2016, 138, 13901−13910

interaction using the ATRaS system, to confirm if ATRaS could be applicable to the analysis of a weaker inhibitor. SERS intensity of Alt-AOMK-modified peptide derived from CatS was around three times lower than that of CatB (Figure S31, Supporting Information), which roughly follows the difference of IC_{50} values between CatB (1.0 μM) and CatS (2.9 μM). This result indicates that Alt-AOMK efficiently forms a covalent bond with CatS. We also performed MALDI mass spectrometry analysis of the ATRaS positive fractions. From the obtained mass spectra, we identified two Alt-AOMK-modified peptides, both derived from the same sequence ^{132}YQGSCGACWAFSAVGALEAQLK^{153}, with different cleavage positions (Table S3, Supporting Information). The results indicate that the Alt-AOMK selectively modified the catalytic site of CatS, similar to that of CatB.

Generally AOMK-containing cysteine protease inhibitors such as Z-FG-AOMK are believed to be covalent-bond-forming inhibitors, but these results obtained by ATRaS experiments suggest that inhibition modes can vary depending on the combination of inhibitors and enzymes. The ATRaS system could provide a new and useful method for the analysis of chemical modification of proteins and insight into the mode of action of small molecules toward target proteins by providing information about binding conditions.

AOMK probe GB111, which has a fluorescence-labeled lysine instead of a glycine of Z-FG-AOMK, was reported to label CatL as well as CatB,[15b] but the labeling selectivity of Z-FG-AOMK itself was not previously investigated. Our measurement indicates that the Alt-AOMK inhibits the activity of CatL, however, the efficiency of covalent bond formation with CatL is more than 1 order of magnitude lower than that with CatB. This result indicates that GB111 labels CatL with the assistance of the interaction between the fluorophore-modified lysine and CatL. In an activity-based proteomics approach, the fluorescent modification of compounds might affect the labeling selectivity as well as the binding affinity.

DISCUSSION

We show here that SERS screening, to find fractions containing modified peptides in a complex proteolytic mixture by using alkyne-tag and SERS spectroscopy, is feasible and offers substantial advantages. For example, if target peptide ions are not detected using the standard comprehensive LC−MS approach with a search engine, it is difficult to know whether the target peptides are actually not present, or whether the ionization conditions are not appropriate for modified peptides. In contrast, our technique, ATRaS, finds specific HPLC fractions containing modified peptides without a priori mass information, regardless of the mode of reaction/modification and the dynamic range of the mass spectrometer; in other words, it pin-points specific fractions for intensive MS analysis and identification of the modified peptides. Both ESI-MS and MALDI-MS are available for the focused analysis of the modified-peptide-containing fractions. The ATRaS system described here offers sufficiently high (nanomolar) sensitivity and reproducibility for use in high-throughput, automated analysis. It reduces the total measurement time for LC−MS, which plays a central role in protein analysis, such as proteomics and high-throughput screening in drug discovery, by identifying the fractions of interest for detailed analysis.

SERS is a powerful technique to overcome the inherently low sensitivity of the Raman scattering spectroscopy. However, poor reproducibility of signal amplitude and spectral shape has limited its practical application in biology, chemical biology and medical science. Specific detection of a target molecule in the presence of many other molecules (such as complex mixture of biomolecules) is particularly challenging, because the conditions of signal amplification in SERS would be determined not only by the parameters regarding light source and size/shape of the nanostructures, but also by the multiple factors such as aggregation state, solvent, contaminant and chemical reactivity of the molecules to the metal surface. At the beginning of our research, we also encountered the problem of reproducibility, but we discovered the conditions for reproducible and efficient SERS detection of alkyne-tagged molecule. Simple addition of TFA greatly improved reproducible aggregation of the commercially available silver nanoparticles in the presence of peptides, which is essential for efficient and stable signal enhancement. It is likely that acidic TFA may uncover the citrates on the surface of silver nanoparticles, and facilitate both the reaction with terminal alkyne and the aggregation of the particles. The silver acetylide formation would play a critical role to concentrate the alkyne tagged molecule to the surface of the nanoparticle.

In ATRaS demonstrated above, the SERS measurement was fully automated by using a computer-controlled scanning stage for changing the target wells in the microtiter plate without manual adjustment of the focus position. The key for the automation is the uniform formation of nanoparticle aggregates by TFA (Figure S17a, Supporting Information). Uniform nanoparticle aggregation at the surface of glass substrate allows us to avoid searching aggregation point manually at each well and to use a constant focal position in SERS detection at each well (Figure S17b and c, Supporting Information). The significant Raman signal amplification of alkyne adsorbed on silver surface shortened the exposure time for SERS detection for 3 s per sample, which corresponds to screening of 96 fractions in 19 min including the dead time of stage scanning of our system (14 min). In principle, the screening time per plate could be reduced to a few seconds by using parallel optical detection. Even under this short exposure time, high sensitivity peptide screening was achieved at femtomole level. To our knowledge, this is the first successful example of the application of SERS for analysis and identification of modified peptides from a complex mixture. There have been some attempts to use SERS detection for HPLC without alkyne-tag, but sensitivity was not high enough to apply it for binding site analysis in combination with mass spectrometry.[18] In the present method, the combination of the alkyne tag and TFA-controlled aggregation of silver nanoparticles enabled us to develop an automated, rapid and semiquantitative analytical system.

In drug discovery and chemical biology researches, identification of amino-acid residue(s), covalently modified with a small molecule is very important to know its specificity, mode of action, and biological importance of the modification. Drugs that form a covalent bond with their target protein such as aspirin and β-lactams have been clinically used, and the efforts to create new covalent drugs have been recently increased.[19] Even in the case of noncovalent drug candidates, affinity labeling, in which amino acid residues near the binding site are selectively and covalently labeled by means of electrophilic or photoactivated reactions, is often used to identify modified amino acid residues with high sensitivity.[1a,3,20] The tiny and bioorthogonal alkyne tag is rapidly emerging as a useful tool for biological research,[17,21] and can be incorporated into various types of biologically important small molecules,[22]

DOI: 10.1021/jacs.6b06003
J. Am. Chem. Soc. 2016, 138, 13901−13910

as well as biomolecules such as nucleic acids,[23] proteins,[24] glycans,[25] and lipids,[6d,26] without affecting their biological activity. These alkyne-tagged molecules are used for the analysis of native chemical modification of proteins such as methylation,[27] acylation,[28] and sugar modification,[25] as well as small molecule metabolism.[29] Alkyne tag is also frequently used in photoaffinity labeling experiments for analyzing protein-small molecule interaction.[30] Normally, the introduction of a secondary tag such as a fluorescent group or biotin by chemical reaction is required for detection, and this has limited the scope of alkyne tag.[21−30] The highly sensitive Raman screening system developed here could provide a novel method to overcome such limitation.

CONCLUSIONS

In conclusion, we have developed ATRaS as an optical screening technique based on the use of alkyne tag in combination with SERS spectroscopy, and applied it to facilitate LC−MS-based analysis of small-molecule-binding site(s) in proteins. Because of its high sensitivity (detection limit: ∼100 femtomole) and quantitative detection capability, ATRaS is a promising tool for direct detection and large-scale screening of alkyne-tagged molecules without the need for any secondary tag, and it is expected to find application in a wide range of research fields, including proteomics, epigenetics, metabolomics and chemical biology.

EXPERIMENTAL SECTION

SERS Analysis of Alkyne-Tagged Synthetic Peptide (Figure 2-4 and S3−S12, S16). Fifteen μL of 40 nm silver nanoparticle solution (EMSC40, British Bio Cell International) was added to a mixture of 14 μL aqueous 0.3% (v/v) trifluoroacetic acid (TFA) solution and 1 μL of aqueous peptide solution (0 or 10 pM ∼ 1 mM) in a glass-bottomed 384-well plate (EZView assay plate, AGC). As standard samples, synthetic peptides EQWPQCPTXK (X = propargyl glycine, alt-pept) and EQWPQCPTIK (pept) were used. The plate was kept for 1 day in the refrigerator at 4 °C, then SERS measurement was performed. As a control experiment without TFA, 15 μL of 40 nm silver nanoparticle solution was added to 14 μL of water mixed with 1 μL of aqueous peptide solution (0 or 1 nM ∼ 1 mM) in the 384-well plate. For SERS measurement, the 384-well plate was set on the Raman microscope stage (Raman-11, Nanophoton). A bright-field image was obtained with halogen lamp illumination. A continuous-wave 532 nm excitation laser was focused as a line at each well by a 0.75 NA dry objective lens (CFI Plan Apo λ 40×, Nikon). Laser power was 240 mW, measured after the objective lens. Exposure time was set as 1 s/line for imaging (25 lines, 25 × 400 pix) or 3 s/line for single line exposure (1 line, 1 × 400 pix). The SERS spectrum of each well was obtained by averaging the SERS image (both imaging and single line). Alkyne intensity was calculated as the difference between peak height of the alkyne at 1958 cm^{-1} and peak bottom intensity. For sensitivity measurement, at each loading amount of peptide, 15 different wells were prepared, and SERS measurement was performed at each well. Laser focus position was set at the upper surface of the glass. The height of laser focus was maintained with autofocus system, correcting focus drift in real-time (Perfect Focus System, Nikon).

LC-SERS Analysis of Alkyne-Tagged Synthetic Peptide (Figure 5 and S13−S15). Ten μL of peptide solution (loading amount was set as 0.3, 1, 3, or 10 pmol) was injected into a nano-LC system (Prominence nano, Shimadzu) with an L-column2 ODS (3 μm, 0.1 × 150 mm, CERI) for analysis and a Zorbax 300SB C18 (5 μm, 5 × 0.3 mm, Agilent) trap column. Elution of peptides was monitored with a UV detector at 215 nm (GL Science, MU701) at a flow rate at 300 nL/min. For the analytical column, mobile phase A (distilled water containing 0.1% (v/v) TFA and 5% (v/v) acetonitrile (MeCN)) and mobile phase B (0.1% (v/v) TFA and 95% (v/v) MeCN) were utilized to form a gradient as follows. 0−60 min: 3−80% B, 60.01−75 min: 95% B, 75.01−105 min 3% B. The eluate was fractionated at 20 s intervals (Probot, Dionnex) into a wells of a glass-bottomed 384 multiwell plate, into which 15 μL of 0.3% (v/v) TFA solution per well had been deposited in advance. Silver nanoparticle solution (15 μL/well) was added to each well, and the plate was kept for 1 day in the refrigerator at 4 °C. Then the 384-well plate was set on the Raman microscope stage. Experimental parameters were the same as in the protocol for SERS analysis of synthetic peptide. The SERS spectrum of each well was automatically obtained by using software that controls the motorized microscope stage, synchronized with excitation laser illumination and CCD camera exposure. Each SERS spectrum was calculated by averaging the SERS images (both single line and imaging). Alkyne intensity was calculated as the difference between alkyne peak height at 1958 cm^{-1} and peak bottom intensity. The laser focus position was maintained with an autofocus system, correcting focus drift in real-time (Perfect Focus System, Nikon).

Sample Preparation of Alt-AOMK-Labeled Cathepsin B (CatB) and Its Trypsin-Digested Peptide Mixture (Figure 6). Human liver CatB (10 μg, CALBIOCHEM) was dissolved in 100 μL of acetate buffer (50 mM sodium acetate (pH 5.6), 5 mM $MgCl_2$, 2 mM dithiothreitol (DTT)), and the solution was kept for 15 min at room temperature. It was then mixed with 1.0 μL of 20 mM Alt-AOMK dissolved in DMSO, and the mixture was incubated for 3 h at 37 °C. After incubation, the proteins in the solution were purified by trichloroacetic acid (TCA) precipitation, with an incubation time of 3 h on ice. Centrifugation was performed at 20 000*g* for 20 min to obtain the precipitate. After removal of the supernatant, 1 mL of acetone was added, and centrifugation was performed at 20 000*g* for 15 min. After removal of acetone, 1 mL of acetone was added again. Centrifugation and acetone treatment was performed three times. The remaining acetone was removed in vacuo for 30 s. The precipitate was dissolved in 20 μL of denaturing buffer (7 M GuHCl, 1 M Tris-HCl (pH 8.5)), and the solution was incubated for 1 h at 37 °C. After reduction and alkylation with DTT and iodoacetamide, trypsin at a concentration of 100 ng/μL was added and incubated for several hours at 37 °C. Approximately 0.01% (w/v) *n*-decyl-β-D-glucopyranoside (DG) (240 μL) was added. Around one-third of the total solution was lyophilized and the residue was dissolved in 50 μL solution (2% MeCN, 0.1% TFA). This whole sample was used for LC-fractionation.

LC-SERS-MS Analysis of Tryptic Digest of Alt-AOMK-Treated CatB (Figure 6, S18). Trypsin-digested peptide mixture of Alt-AOMK-labeled CatB was fractionated on a Nano Frontier nLC (Hitachi High-Technologies) equipped with a MU701 UV detector. Peptides were separated on a L-column2 ODS (3 μm, 0.1 × 150 mm, CERI) with a monolithic trap column C18−50−150 (50 μm, 0.05 × 150 mm, Hitachi High-Technologies) at flow rate of 250 nL/min. The UV chromatogram was obtained with a UV detector (MU701, GL Science) set at 215 nm. For the analytical column, mobile phase A (distilled water containing 0.1% (v/v) TFA and 2% (v/v) MeCN) and mobile phase B (0.08% (v/v) TFA and 98% (v/v) MeCN) were utilized to prepare a gradient as follows. 0−60 min: 5−80%, 60.01−75 min: 95% B, 75.01−105 min 5% B. The eluate was fractionated into a glass-bottomed 384-well plate, preloaded with 25 μL of 0.1% (v/v) TFA solution in each well, via a fraction collector at 20 s intervals. The 25 μL solution was divided into two portions of 15 μL (for SERS) and 10 μL (for LC−MS). In the case of the 15 μL solution for SERS, 15 μL of silver nanoparticle solution was added to each well, and the plate was kept for 1 day in the refrigerator at 4 °C. The 384-well plate was set on the Raman microscope stage. Experimental parameters and procedures were the same as in the protocol described for LC-SERS analysis of alkyne-tagged synthetic peptide, except for the laser power, which was set at 130 mW. The SERS spectrum of each well was obtained by averaging SERS images (1 line, 1 × 400 pixels). Alkyne intensity was calculated as the difference of alkyne peak height at 1981 cm^{-1} and peak bottom intensity. For LC−MS, 10 μL of target fraction from the position indicated by the SERS chromatogram was used.

LC−MS and Data Analysis (Figure 6, Figure S18−S19, S22−S23, Table 1). All solvents for LC−MS analysis, including TFA, distilled water containing 0.1% (v/v) formic acid (FA) and MeCN containing 0.1% (v/v) FA, were purchased from Kanto Chemical Co.,

DOI: 10.1021/jacs.6b06003
J. Am. Chem. Soc. 2016, 138, 13901−13910

Inc. LC−MS analysis was performed using a nanoflow HPLC system (UltiMate 3000, Thermo Fisher Scientific, Inc.) and a LTQ Orbitrap XL mass spectrometer (Thermo Fisher Scientific, Inc.) equipped with an electrospray ionization (ESI) source in the positive mode. For automatic measurement and data analysis, Xcalibur software was used (Thermo Fisher Scientific, Inc.). Peptides were separated on a capillary column (0.075 × 100 mm, NTCC-360/75−3−10, Nikkyo Technos Co., Ltd.) as an analytical column with a trap column (ZORBAX 300SB-C18, 0.3 × 5 mm, Agilent Technologies, Inc.). Elution of peptides was done with mobile phase A (distilled water containing 0.1% (v/v) FA and 4% (v/v) MeCN) and mobile phase B (MeCN containing 0.1% (v/v) FA) at a flow rate of 250 nL/min. A representative gradient used in LC−MS experiments was as follows. 0−10 min: 0% B, 10−58 min: 70% B, 59−64 min: 100% B, 65−80 min: 0% B. In order to achieve high recovery of samples from the 384-well plate (AB-1056, Thermo Fisher Scientific, Inc.) (Figure S20, 10 μL for LC−MS) or the ITOP plate, the wells or spots were washed with a small amount of 70% (v/v) FA solution and 0.01−0.05% (w/v) DG solution after recovery of the sample solution.[31] MS/MS data were submitted for database searching by the MASCOT (www.matrixscience.com) search engine installed in-house via Proteome Discoverer software (Thermo Fisher Scientific, Inc.). The representative Mascot MS ion search parameters were as follows: ± 0.8 Da fragment mass tolerance; ± 10 ppm peptide mass tolerance; trypsin enzyme specificity (up to three missed cleavages); variable modifications of methionine oxidation (15.99491 Da), carbamidomethylation on cysteine (57.02146 Da), or alternatively modification on cysteine by Alt-AMOK (376.142307 Da) or Alexa Fluor 488-Alt-AOMK (1034.257490 Da).

Sample Preparation of Alt-AOMK-Treated Cell Lysate Containing CatB and Its Trypsin-Digestion (Figure 8). Cell lysate was prepared from HL-60 cells. HL-60 cells (4.2×10^7 cells) were collected, washed with PBS, then lysed by 1.4 mL of cell lysis buffer (cathepsin B activity fluorometric assay kit, K140−100, BioVision). After centrifugation at 15 000*g* for 10 min, supernatant was obtained as cell lysate, in which protein concentration was determined by Quick Start Bradford Assay kit (BIORAD) as 0.93 mg/mL. 22.5 μg of cell lysate solution was mixed with 2.5 μg of CatB (CALBIOCHEM), and dissolved in 100 μL of acetate buffer (50 mM sodium acetate (pH 5.6), 5 mM $MgCl_2$, 2 mM dithiothreitol (DTT)), and the solution was kept for 15 min at room temperature. It was then mixed with 1.0 μL of 20 mM Alt-AOMK dissolved in DMSO, and the mixture was incubated for 3 h at 37 °C. After incubation, the proteins in the solution were purified by TCA precipitation, with an incubation time of 3 h on ice. Centrifugation was performed at 20 000*g* for 20 min to obtain the precipitate. After removal of the supernatant, 1 mL of acetone was added, and centrifugation was performed at 20 000*g* for 15 min. After removal of acetone, 1 mL of acetone was added again. Centrifugation and acetone treatment was performed three times. The remaining acetone was removed in vacuo for 30 s. The precipitate was dissolved in 20 μL of denaturing buffer, and the solution was incubated for 1 h at 37 °C. After reduction and alkylation with DTT and iodoacetamide, trypsin at a concentration of 100 ng/μL was added and incubated for several hours at 37 °C. Approximately 0.01% (w/v) DG (240 μL) was added. Around one-tenth of the total solution was used for LC-fractionation.

LC-SERS-MS Analysis of the Trypsin-Digest of Cell Lysate Containing CatB (Figure 8). Trypsin-digested peptide mixture of Alt-AOMK-treated cell lysate containing CatB was fractionated on an UltiMate 3000 RSLC nano system (Thermo scientific) equipped with a MU701 UV detector (GL Science). Peptides were separated on an Acclaim PepMap RSLC (C18, 2 μm, 0.075 × 150 mm, Thermo scientific) as an analytical column with an Acclaim PepMap μ-precolumns (C18, 5 μm, 0.3 × 5 mm, Thermo scientific) as a trap column at flow rate of 250 nL/min. The UV chromatogram was obtained at 215 nm. For HPLC solvent, mobile phase A (distilled water containing 0.1% (v/v) TFA) and mobile phase B (0.1% (v/v) TFA and 90% (v/v) MeCN) were utilized to prepare a gradient as follows. 0−10 min: 4% B, 10−65 min 4−44% B, 65−109 min: 44−99% B, 109−114 min: 99% B, 114−115 min 99−4% B, 115−125 min 4% B. The eluate was fractionated into a glass-bottomed 384-well plate, preloaded with 25 μL of 0.3% (v/v) TFA solution in each well, via a fraction collector at 20 s intervals. Thirty μL of silver nanoparticle solution was added to each well, and the plate was kept for 1 day in the refrigerator at 4 °C. The 384-well plate was set on the Raman microscope stage. Experimental parameters and procedures were the same as in the protocol described for LC-SERS analysis of alkyne-tagged synthetic peptide, except for the laser power, which was set at 460 mW and exposure time, which was set at 5 s/line (1 × 400 pix). The SERS spectrum of each well was obtained by averaging SERS image (1 line, 1 × 400 pixels). Alkyne intensity was calculated as the difference of alkyne peak height at 1981 cm^{-1} and peak bottom intensity. For MALDI-TOF MS, supernatant of the target fraction was removed, and 1 μL of 0.01% DG and 1 μL of MeCN was added in the well. The precipitated sample on the substrate was collected in the solution by scratching surface of the substrate with pipet apex. All the sample solution was deposited on the MALDI plate, and mixed with α-cyano-4-hydroxycinnamic acid (CHCA, Bruker Daltonics) as a matrix. MALDI-TOF MS measurement was performed with an autoflex speed TOF/TOF (Bruker Daltonics).

■ ASSOCIATED CONTENT

Supporting Information

The Supporting Information is available free of charge on the ACS Publications website at DOI: 10.1021/jacs.6b06003.

Details of the experimental procedures for Raman analysis of alkyne-tagged synthetic peptide, sample preparation of Alt-AOMK-labeled CatB with and without click reaction, comparison between SERS detection and click-chemistry-based fluorescence detection, cathepsin inhibition assay, syntheses of compounds, sample preparation and LC-SERS-MS analysis of tryptic digest of the Alt-AOMK-treated cell lysate containing CatB, sample preparation and LC-SERS-MS of Alt-AOMK-labeled CatB, CatL and CatS, and MALDI-TOF MS analysis of peptides after SERS (PDF)

■ AUTHOR INFORMATION

Corresponding Authors

*fujita@ap.eng.osaka-u.ac.jp

*sodeoka@riken.jp

Notes

The authors declare no competing financial interest.

■ ACKNOWLEDGMENTS

We acknowledge RIKEN BSI Research Resources Center for technical help, and thank M. Usui for assistance with HPLC. We also thank T. Ota (Nanophoton) for development of the Raman microscope, D. Higo (Thermo Fisher Scientific) for advice on mass spectrometric analysis and S. Kamisuki (Azabu University) for optimizing the CatB reaction conditions. This work was partially supported by JST, AMED, RIKEN, JSPS KAKENHI Grant Number 26600117 (J.A.), and JSPS KAKENHI Grant Number 23710276 (H.Y.).

■ REFERENCES

(1) (a) Al-Mawsawi, L. Q.; Fikkert, V.; Dayam, R.; Witvrouw, M.; Burke, T. R., Jr.; Borchers, C. H.; Neamati, N. *Proc. Natl. Acad. Sci. U. S. A.* **2006**, *103*, 10080−10085. (b) Buey, R. M.; Calvo, E.; Barasoain, I.; Pineda, O.; Edler, M. C.; Matesanz, R.; Cerezo, G.; Vanderwal, C. D.; Day, B. W.; Sorensen, E. J.; López, J. A.; Andreu, J. M.; Hamel, E.; Díaz, J. F. *Nat. Chem. Biol.* **2007**, *3*, 117−125. (c) Mertins, P.; Qiao, J. W.; Patel, J.; Udeshi, N. D.; Clauser, K. R.; Mani, D. R.; Burgess, M.

DOI: 10.1021/jacs.6b06003
J. Am. Chem. Soc. 2016, 138, 13901−13910

W.; Gillette, M. A.; Jaffe, J. D.; Carr, S. A. *Nat. Methods* **2013**, *10*, 634−637.
(2) (a) Cravatt, B. F.; Wright, A. T.; Kozarich, J. W. *Annu. Rev. Biochem.* **2008**, *77*, 383−414. (b) Fonović, M.; Bogyo, M. *Expert Rev. Proteomics* **2008**, *5*, 721−730. (c) Heal, W. P.; Dang, T. H.; Tate, E. W. *Chem. Soc. Rev.* **2011**, *40*, 246−257. (d) Speers, A. E.; Adam, G. C.; Cravatt, B. F. *J. Am. Chem. Soc.* **2003**, *125*, 4686−4687. (e) Willems, L. I.; Overkleeft, H. S.; van Kasteren, S. I. *Bioconjugate Chem.* **2014**, *25*, 1181−1191.
(3) Calvo, E.; Camafeita, E.; Diaz, J. F.; Lopez, J. A. *Curr. Proteomics* **2008**, *5*, 20−34.
(4) Han, X.; Aslanian, A.; Yates, J. R., III. *Curr. Opin. Chem. Biol.* **2008**, *12*, 483−490.
(5) Sadaghiani, A. M.; Verhelst, S. H.; Bogyo, M. *Curr. Opin. Chem. Biol.* **2007**, *11*, 20−28.
(6) (a) Yamakoshi, H.; Dodo, K.; Okada, M.; Ando, J.; Palonpon, A.; Fujita, K.; Kawata, S.; Sodeoka, M. *J. Am. Chem. Soc.* **2011**, *133*, 6102−6105. (b) Yamakoshi, H.; Dodo, K.; Palonpon, A.; Ando, J.; Fujita, K.; Kawata, S.; Sodeoka, M. *J. Am. Chem. Soc.* **2012**, *134*, 20681−20689. (c) Palonpon, A. F.; Ando, J.; Yamakoshi, H.; Dodo, K.; Sodeoka, M.; Kawata, S.; Fujita, K. *Nat. Protoc.* **2012**, *8*, 677−692. (d) Ando, J.; Kinoshita, M.; Cui, J.; Yamakoshi, H.; Dodo, K.; Fujita, K.; Murata, M.; Sodeoka, M. *Proc. Natl. Acad. Sci. U. S. A.* **2015**, *112*, 4558−4563.
(7) (a) Jeanmaire, D. L.; Van Duyne, R. P. *J. Electroanal. Chem. Interfacial Electrochem.* **1977**, *84*, 1−20. (b) Moskovits, M. *Rev. Mod. Phys.* **1985**, *57*, 783−826. (c) Jackson, J. B.; Halas, N. J. *Proc. Natl. Acad. Sci. U. S. A.* **2004**, *101*, 17930−17935.
(8) Long, N. J.; Williams, C. K. *Angew. Chem., Int. Ed.* **2003**, *42*, 2586−2617.
(9) (a) Manzel, K.; Schulze, W.; Moskovits, M. *Chem. Phys. Lett.* **1982**, *85*, 183−186. (b) Feilchenfeld, H.; Weaver, M. J. *J. Phys. Chem.* **1989**, *93*, 4276−4282. (c) Joo, S.-W.; Kim, K. *J. Raman Spectrosc.* **2004**, *35*, 549−554. (d) Song, Z.-L.; Chen, Z.; Bian, X.; Zhou, L.-Y.; Ding, D.; Liang, H.; Zou, Y.-X.; Wang, S.-S.; Chen, L.; Yang, C.; Zhang, X.-B.; Tan, W. *J. Am. Chem. Soc.* **2014**, *136*, 13558−13561.
(10) (a) Kneipp, K.; Kneipp, H.; Kneipp, J. *Acc. Chem. Res.* **2006**, *39*, 443−450. (b) Guerrini, L.; Graham, D. *Chem. Soc. Rev.* **2012**, *41*, 7085−7107.
(11) (a) Hamada, K.; Fujita, K.; Smith, N.; Kobayashi, M.; Inouye, Y.; Kawata, S. *J. Biomed. Opt.* **2008**, *13*, 044027. (b) Fujita, K.; Ishitobi, S.; Hamada, K.; Smith, N. I.; Taguchi, A.; Inouye, Y.; Kawata, S. *J. Biomed. Opt.* **2009**, *14*, 024038.
(12) (a) Zheng, C. J.; Han, L. Y.; Yap, C. W.; Ji, Z. L.; Cao, Z. W.; Chen, Y. Z. *Pharmacol. Rev.* **2006**, *58*, 259−279. (b) Withana, N. P.; Blum, G.; Sameni, M.; Slaney, C.; Anbalagan, A.; Olive, M. B.; Bidwell, B. N.; Edgington, L.; Wang, L.; Moin, K.; Sloane, B. F.; Anderson, R. L.; Bogyo, M. S.; Parker, B. S. *Cancer Res.* **2012**, *72*, 1199−1209.
(13) Mohamed, M. M.; Sloane, B. F. *Nat. Rev. Cancer* **2006**, *6*, 764−775.
(14) Smith, R. A.; Copp, L. J.; Coles, P. J.; Pauls, H. W.; Robinson, V. J.; Spencer, R. W.; Heard, S. B.; Krantz, A. *J. Am. Chem. Soc.* **1988**, *110*, 4429−4431.
(15) (a) Kato, D.; Boatright, K. M.; Berger, A. B.; Nazif, T.; Blum, G.; Ryan, C.; Chehade, K. A. H.; Salvesen, G. S.; Bogyo, M. *Nat. Chem. Biol.* **2005**, *1*, 33−38. (b) Blum, G.; Mullins, S. R.; Keren, K.; Fonovic, M.; Jedeszko, C.; Rice, M. J.; Soloane, B. F.; Bogyo, M. *Nat. Chem. Biol.* **2005**, *1*, 203−209.
(16) Evans, M. J.; Cravatt, B. F. *Chem. Rev.* **2006**, *106*, 3279−3301.
(17) Thirumurugan, P.; Matosiuk, D.; Jozwiak, K. *Chem. Rev.* **2013**, *113*, 4905−4979.
(18) (a) Freeman, R. D.; Hammaker, R. M.; Meloan, C. E.; Fateley, W. G. *Appl. Spectrosc.* **1988**, *42*, 456−460. (b) Ni, F.; Sheng, R.; Cotton, T. M. *Anal. Chem.* **1990**, *62*, 1958−1963. (c) Sheng, R.; Ni, F.; Cotton, T. M. *Anal. Chem.* **1991**, *63*, 437−442. (d) Cabalin, L. M.; Ruperez, A.; Laserna, J. J. *Talanta* **1993**, *40*, 1741−1747. (e) Cabalin, L. M.; Ruperez, A.; Laserna, J. *Anal. Chim. Acta* **1996**, *318*, 203−210. (f) Carrillo-Carrión, C.; Armenta, S.; Simonet, B. M.; Valcárcel, M.; Lendl, B. *Anal. Chem.* **2011**, *83*, 9391−9398.
(19) (a) Singh, J.; Petter, R. C.; Baillie, T. A.; Whitty, A. *Nat. Rev. Drug Discovery* **2011**, *10*, 307−317. (b) Cohen, M. S.; Zhang, C.; Shokat, K. M.; Tauton, J. *Science* **2005**, *308*, 1318−1321.
(20) Robinette, D.; Neamati, N.; Tomer, K. B.; Borchers, C. H. *Expert Rev. Proteomics* **2006**, *3*, 399−408.
(21) (a) Bertozzi, C. R.; Boyce, M. *Nat. Methods* **2011**, *8*, 638−642. (b) Grammel, M.; Hang, H. C. *Nat. Chem. Biol.* **2013**, *9*, 475−483.
(22) Hoffstrom, B. G.; Kaplan, A.; Letso, R.; Schmid, R. S.; Turmel, G. J.; Lo, D. C.; Stockwell, B. R. *Nat. Chem. Biol.* **2010**, *6*, 900−906.
(23) (a) Salic, A.; Mitchison, T. *Proc. Natl. Acad. Sci. U. S. A.* **2008**, *105*, 2415−2420. (b) Jao, C. Y.; Salic, A. *Proc. Natl. Acad. Sci. U. S. A.* **2008**, *105*, 15779−15784. (c) Limsirichaikul, S.; Niimi, A.; Fawcett, H.; Lehmann, A.; Yamashita, S.; Ogi, T. *Nucleic Acids Res.* **2009**, *37*, e31.
(24) (a) Best, M. D. *Biochemistry* **2009**, *48*, 6571−6584. (b) Lang, K.; Chin, J. W. *Chem. Rev.* **2014**, *114*, 4764−4806. (c) Deiters, A.; Cropp, T. A.; Mukherji, M.; Chin, J. W.; Anderson, J. C.; Schultz, P. G. *J. Am. Chem. Soc.* **2003**, *125*, 11782−11783. (d) Szychowski, J.; Mahdavi, A.; Hodas, J. J. L.; Bagert, J. D.; Ngo, J. T.; Landgraf, P.; Dieterich, D. C.; Shuman, E. M.; Tirrell, D. A. *J. Am. Chem. Soc.* **2010**, *132*, 18351−18360.
(25) (a) Chang, P. V.; Chen, X.; Smyrniotis, C.; Xenakis, A.; Hu, T.; Bertozzi, C. R.; Wu, P. *Angew. Chem., Int. Ed.* **2009**, *48*, 4030−4033. (b) Soriano Del Amo, D.; Wang, W.; Jiang, H.; Besanceney, C.; Yan, A. C.; Levy, M.; Liu, Y.; Marlow, F. L.; Wu, P. *J. Am. Chem. Soc.* **2010**, *132*, 16893−16899.
(26) Martin, B. R.; Wang, C.; Adibekian, A.; Tully, S. E.; Cravatt, B. F. *Nat. Methods* **2012**, *9*, 84−89.
(27) (a) Bothwell, I. R.; Islam, K.; Chen, Y.; Zheng, W.; Blum, G.; Deng, H.; Luo, M. *J. Am. Chem. Soc.* **2012**, *134*, 14905−14912. (b) Shimazu, T.; Barjau, J.; Sohtome, Y.; Sodeoka, M.; Shinkai, Y. *PLoS One* **2014**, *9*, e105394.
(28) (a) Hang, H. C.; Wilson, J. P.; Charron, G. *Acc. Chem. Res.* **2011**, *44*, 699−708. (b) Yang, Y.-Y.; Ascano, J. M.; Hang, H. C. *J. Am. Chem. Soc.* **2010**, *132*, 3640−3641.
(29) El-Mashtoly, S. F.; Petersen, D.; Yosef, H. K.; Mosig, A.; Reinacher-Schick, A.; Kötting, C.; Gerwert, K. *Analyst* **2014**, *139*, 1155−1161.
(30) Peng, T.; Yuan, X.; Hang, H. C. *Curr. Opin. Chem. Biol.* **2014**, *21*, 144−153.
(31) (a) Tomita, T.; Mizumachi, Y.; Chong, K.; Ogawa, K.; Konishi, N.; Sugawara-Tomita, N.; Dohmae, N.; Hashimoto, Y.; Takio, K. *J. Biol. Chem.* **2004**, *279*, 54161−54172. (b) Kodama, K.; Fukuzawa, S.; Nakayama, H.; Kigawa, T.; Sakamoto, K.; Yabuki, T.; Matsuda, N.; Shirouzu, M.; Takio, K.; Tachibana, K.; Yokoyama, S. *ChemBioChem* **2006**, *7*, 134−139.

DOI: 10.1021/jacs.6b06003
J. Am. Chem. Soc. 2016, 138, 13901−13910